STUDY OF THE EFFECTS OF SELENIUM NANOPARTICLES AND THEIR COMBINATION WITH IMMUNOGLOBULINS ON THE SURVIVAL AND FUNCTIONAL STATE OF POLYMORPHONUCLEAR CELLS

D.A. Serov[1,2*], *V.V. Khabatova*[1], *I.V. Tikhonova*[1,2], *V.E. Reut*[3], *R.V. Pobedonostsev*[1], *M.E. Astashev*[1,2]

[1] Prokhorov General Physics Institute of the Russian Academy of Sciences, 38 Vavilov St., Moscow, 119991, Russia;
[2] Institute of Cell Biophysics of the Russian Academy of Sciences, Institutskaya str. 3, Pushchino, Moscow region, 142290, Russia;
[3] Belarusian State University, 4 Nezavisimosti Av., Minsk, 220030, Belarus.

* Corresponding author: dmitriy_serov_91@mail.ru

Abstract. Selenium and its compounds are promising immunomodulatory agents. We studied the ability of selenium nanoparticles (Se NPs) and their combination with immunoglobulins (IgG) to influence the functional responses of immune cells and the expression profile of "stress associated". The cytotoxic effect of Se NPs was also studied in primary and immortalized cell cultures. Se NPs were obtained by laser ablation in water followed by fragmentation. Fragmentation control was performed using acoustic and optical methods of size estimation. The size distribution of Se NPs was narrow and an average size was 100 nm. The Se NPs did not exhibit cytotoxicity against fibroblasts, hepatocytes and cell line L-929. Weak cytotoxicity was found for the HL-60 granulocyte-like culture. On a surviving culture of mouse granulocytes, no cytotoxic effect was found. The addition of Se NPs in combination with IgG can modulate the maximum and total production of ROS by murine granulocytes induced by W-peptide and PMA and modulate the proportion of granulocytes with calcium responses to Wp. Se NPs modulate the action of IgG on the physiological responses of granulocytes. In the study of gene expression, similar patterns were found. Se NPs increase the expression of *HSP90, NFkb, Xrcc4, SOD2* genes; IgG enhances the effect of Se NPs, while IgG decreased the expression of these genes. This phenomenon can be explained by the interaction between Se NPs and IgG. Data of spectral methods showed the binding of IgG to Se NP surface and a partial change in the spatial structure of IgG.

Keywords: selenium nanoparticles, immunoglobulin, laser fragmentation, innate immune cells, reactive oxygen species, gene expression, calcium activity of non-excitable cells.

List of Abbreviations

DLS – dynamic light scattering
FPR2 – receptors of formylated peptides 2
IgG – immunoglobulin G
IP3 – inositol triphosphate
GPCR – G protein-coupled receptor
LED – light emitting diode
NETs – neutrophil extracellular traps
NF-κB – nuclear transcription factor κB
NP – nanoparticles
PBS – phosphate-buffered saline
PIP2 – phosphatidylinositol 4,5-bisphosphate
PLC-β – phospholipase C
PKC – protein kinase C
PMA – phorbol myristate acetate
ROS – reactive oxygen species
RT PCR – reverse transcription polymerase chain reaction
TEM – transmission electron microscopy
Wp – peptide WKYMVM

Introduction

Polymorphonuclear cells (granulocytes) are a population of leukocytes with a large segmented nucleus and specific granules in cytoplasm. Among the granulocytes, three large subpolations (neutrophils, eosinophils and basophils) are distinguished, depending on the characteristics of granules staining (Lin & Loré, 2017). In most cases, the granules are large or altered lysosomes and peroxisomes (Fingerhut *et al.*, 2020). Granulocytes play key role in innate immune responses. They provide primary protection against infectious agents or host's cancrine cells. Granulocytes are also involved in the regulation of processes associated with

the regulation of inflammation (Peiseler & Kubes, 2019). Granulocytes can eliminate a pathogen via two groups of mechanisms. The first group of mechanisms includes phagocytosis, accelerated reactive oxygen species (ROS) generation "respiratory burst", release of neutrophil extracellular traps (NETs) (Stoiber *et al.*, 2015). The second group of mechanisms mainly associated with the secretion of a large number of different signal molecules, including cytokines (Lehman & Segal, 2020). The functioning of granulocytes is usually accompanied by migration to the site of inflammation (Phillipson & Kubes, 2011).

The functioning of granulocytes, like any other immune cells, must be strictly regulated. Regulation occurs via small signaling molecules and proteins, including immunoglobulins (Chiu *et al.*, 2019; Gál *et al.*, 2017; Vinolo *et al.*, 2011). In the case of pathological processes (autoimmune disorders and oncology), the regulation of granulocyte functioning may be disturbed. In this case, granulocytes can cause serious damage of tissues and organs due to excessive cytotoxic activity, overproduction of ROS and the development of chronic inflammation due to improper functioning of the NET system (Galvão *et al.*, 2019; Kang *et al.*, 2021).

Selenium is essential microelement for living organisms. The human body contains about 10–14 mg of selenium, and human's daily need for selenium is 70–100 μg/day (Janghorbani *et al.*, 1990). Selenium is involved in maintaining an adequate redox balance in a cell and participates in the regulation of metabolism. Selenium is included in amino acids selenocysteine. This amino acid plays key role the functioning active sites of enzymes (Zhang *et al.*, 2022). Selenium promotes the assimilation of iodine, acts as antioxidant (Siddik *et al.*, 2022; Veisa *et al.*, 2021). In addition, the radioprotective and radiomitigatory properties of selenium are described (Gudkov *et al.*, 2015; Proshin *et al.*, 2017). It is described, that selenium deficiency interferes immune system functions (Guillin *et al.*, 2019). The adequate intake of selenium is important for adequate activity of most cells of innate immunity (Xia *et al.*, 2021; Zhang *et al.*, 2021). A supposed mechanism of immunomod-ulatory activity of selenium is its antioxidant properties. In some case, selenium is can prevent the development of oxidative stress and protect cells from damage to nucleic acids, proteins, and other biomolecules by reactive species (Kuropatkina *et al.*, 2022; Varlamova *et al.*, 2021b). At the present day, scientists pay great attention on nanoscale forms of selenium: selenium nanoparticles (Se NPs) and nanofibers. Selenium nanoparticles can be used in biomedicine and agriculture (Bora *et al.*, 2022; Varlamova *et al.*, 2021c). Nanoparticles commonly consist of selenium in nonoxidased form Se^0, which is insoluble in water. Selenium can slowly oxidize and transform into selenium oxides, which are highly soluble in water and are able to quickly enter into biological cycles (Khurana *et al.*, 2019). Therefore, Se NPs can show significant toxicity and create a powerful prolonged effect on living systems (Hosnedlova *et al.*, 2018). Se NPs show more toxicity against cancer cells compared to normal cells (Varlamova *et al.*, 2021a). In addition, Se NPs have chemical stability and can to adsorb a lot of small molecules on threir surface. These properties made Se NPs a candidate for the manufacture of drug delivery systems (Maiyo & Singh, 2017). The size of 50–100 nm is a significant competitive advantage of selenium nanoparticles, since, due to the size, Se NPs are not absorbed by the reticuloendothelial system, and they are not filtered out in the kidneys (Hosnedlova *et al.*, 2018). Se NPs can modulate activity of immune cells, for example, production of cytokines by macrophages (Pi *et al.*, 2020). There are data about potential using of Se NPs to reduce the growth and development of tumors via activating specific T-cells and tumor-associated macrophages (Gautam *et al.*, 2017). Se NPs are also being considered for the role of an agent preventing immunosuppression in chemotherapy. It has been shown that in cytoxan-induced immunosuppression, daily intake of Se NPs in a polymeric carbohydrate matrix stimulated the production of immune factors by immune cells (Dung *et al.*, 2021).

Immunosuppression during chemotherapy seriously increases the risk of developing infec-tious diseases in cancer patients. Moreover, in-fections can be caused by including opportunistic pathogens. There are a sufficient number of works in which Se NPs is considered as a universal new therapeutic agent for neutralizing immune system dysfunction in bacterial infections, cancer, and immunosuppression-associated pathologies (Ferro *et al.*, 2021; Gao *et al.*, 2021; Zeng *et al.*, 2021).

In general, a lot is known about the immunomodulatory properties of Se NPs. This study is mainly focused on the modulation of the physiological state of granulocytes due to Se NPs, as well as the ability of Se NPs themselves and in combination with antibodies to influence the innate immune cell functional status.

Materials and Methods

Selenium nanoparticles fabrication

Se NPs were obtained by laser ablation followed by laser fragmentation. Solid Se (Sigma Aldrich) was used as a target. Ytterbium-doped fiber laser (YLPM-1) with wavelength 1060-1070 nm was used to ablation and fragmentation. Laser pulses had average power 20 mV, duration 80 ns and repetition 20 kHz. More detailed description can be found in previous work (Simakin *et al.*, 2021).

Animals

The study was performed on male 8-10 weeks old BALB/c mice weighing 21-24 g. The animals were purchased at the Stolbovaya Nursery (Stolbovaya Branch of the Scientific Biomedical Technology Centre of the Federal Medico-Biological Agency (Moscow region, Russia)). All procedures of primary cells isolation performed in accordance with the European Communities Council Directive (November 24, 1986; 86/609/EEC) and the Declaration on Humane Treatment of Animals. The protocol of experiments was approved by the Commission on Bioethics (no. 12306, 2006) of the Institute of Cell Biophysics of Russian Academy of Sciences. The animals received drink and feed *accesso libero*.

Bone marrow granulocytes isolation

Isolation of granulocytes from mouse bone marrow was performed by centrifugation on a percoll density gradient according to the standard method (Filina *et al.*, 2014). Mice were immobilized by cervical dislocation. The femur, tibia and ulna were extracted, the epiphyses were cut off and washed with RPMI-1640 (Gibco, USA). The cell suspension was layered on a Percoll gradient in PBS (78%, 62.5%, 55%, vol/vol) and centrifuged at 1500 g, 35 min, 4 ℃. The cells were collected from the border of 62.5% and 78%, washed in RPMI-1640, then in PBS and diluted in a Hanks solution without calcium to a concentration of 10^7 cells/ml. The cells were kept on ice for 1 hour for resting.

The survival of the obtained cells was evaluated by trypan blue staining. The polymorphic morphology of nucleus was confirmed by Hoechst 33258 staining, maturity was evaluated by staining with PE-conjugated monoclonal anti-Ly-6G/Ly-6C (Gr-1) antibodies (ThermoFisher, USA) clone RB6-8C5. The evaluation was performed using a DM 6000 fluorescence microscope (Leica, Germany). Samples of cells with a survival rate at least 98% and a proportion of polymorphonuclear and Gr-1^+ cells at least 90% were taken into the experiment.

ROS production measurement

Concentration of ROS production by granulocytes were evaluated by chemiluminescent method using chemiluminometer Chemilum-12 (IBC RAS, Pushchino, Russia). Samples (2×10^6 cells in 200 μl a Hanks solution with 1 mM calcium chloride) were incubated in measuring wells during 20 min at 37 °C in the presence of 0.35 mm luminol, 0.1 mm NaN_3, 1 u/ml horseradish peroxidase type IV, pH 7.38. After incubation, the samples were placed in a chemiluminometer measuring chamber. The baseline of luminescence level was recorded for 4 minutes. Further the corresponding stimulus 10^{10}/ml Se NP and/or 0.5 mg/ml of polyclonal human immunoglobulins IgG (Microgen, Russia) was added, luminescence was recorded for 20 minutes, after which respiratory explosion

inducers were added: 1 μM synthetic peptide WKYMVM (Wp) or protein kinase C (PKC) activator 1 μM phorbol myristate acetate (PMA) (Hao *et al.*, 2020; Sokolov *et al.*, 2018). The intensity of chemiluminescence of cells was recorded for 250 seconds. Each sample was measured in duplicates. A detailed description of the experimental procedures can be found in the previous work (Safronova *et al.*, 2021).

Assay of granulocytes calcium activity

The concentration of calcium cations in the cytoplasm of murine granulocytes was evaluated by fluorescence microscopy. Granulocytes (10^6 cells/ml in a drop of 100 μl Hanks solution) were applied to a round cover glass Ø 25 mm, placed in a wet chamber and incubated during 15 min at 37 ℃ for adhesion.

Further cells were loaded by Fura2-AM ratiometric fluorescent dye (ThermoFisher, USA) 45 min at 37 ℃ in a wet chamber. Cover glasses with cells were placed in commercially available chamber-holder RC-40LP (Warner Instruments, USA). The cells were immediately washed twice with 1 ml of a complete Hanks solution preheated to 37 ℃, 1 ml of a heated Hanks solution was added to the washed cells and placed on a thermostatically controlled objective table at 37 ℃.

Fluorescent signals were recorded using an imaging installation based on an inverted AE31E microscope (Motic, Spain), an SDU-285 digital camera (SpecTeleTechnika, Russia) and an LED lighting system. Fura 2AM fluorescence was recorded in radiometric mode at wavelengths of exciting light of 340 and 380 nm. The concentration of calcium in the cytoplasm of granulocytes was estimated by the ratio of fluorescence F340/F380. Background values of fluorescence intensity were preliminary subtracted in each sample before analysis (Turovsky *et al.*, 2012). The settings of the current strength of the LED illuminator, the exposure time and gain were constant for all variants of the experiment.

Cell fluorescence was recorded at base conditions during 4 minutes, then 10^{10}/ml Se NP, 0.5 mg/ml IgG or a combination thereof were added in appropriate samples. Further fluorescence was recorded for 15 minutes, then the proinflammatory agent W-peptide (1 μM) was added in each sample and fluorescence were recorded for 5 minutes. In control samples, sterile PBS was used as the first additive. WinFluorXE acquisition software (J. Dempster, Strathclyde Electrophysiology Software, University of Strathclyde, UK) was used for data collection. A more detailed description of the measuring setup, data collection mode can be found in the previous work (Serov *et al.*, 2021).

Calcium activity of cells was evaluated as by the proportion of cells with calcium responses in the total population after each addition. This approach is based on the calculation of skewness (asymmetry, *As*) of the F340/F380 values for each cell under each experimental conditions. This method was developed by us earlier to evaluate the calcium activity of electrically non-excitable cells. A detailed description of the principle of the method can be found in study (Serov *et al.*, 2019).

Micronucleus Assay

Cytogenetic damage of cells was assessed by the proportion of polychromatophilic red cells with micronucleus in all population of polychromatophilic red cells. Isolation of red bone marrow, obtaining of preparations for microscopy and their staining are described in detail in the previous work (Sharapov *et al.*, 2017). The maximum yield of polychromatophilic red cells with micronucleus is observed about a day after exposure. Therefore samples were prepared after 24 hours of nanoparticles influence. The counting of polychromatophilic red cells with micronucleus was carried out using a light microscope with an immersion lens at a magnification of ×1000. Details are described earlier (Gudkov *et al.*, 2009).

Cytotoxicity assay

Acute cytotoxicity studies were performed using standard *in vitro* test systems: primary cultures of mouse hepatocytes and fibroblasts, as well as permanent cell lines L929 (mouse connective tissue, ATCC №CCL-1) and HL-60 (human leukemia cells, ATCC № CCL-240). The cells were grown in DMEM (Biolot, Rus-

Table 1

Primers used for qRT-PCR

№	Genes	GenBank accsession #	Oligonucleotide 5'-3'	Amplicon Size, bp
1	*Actb*	NM_007393.4	CCTTCCTTCTTGGGTATGGAATCC	115
			CACCAGACAGCACTGTGTTGGCA	
2	*HSP90*	NM_011631	GTCCGCCGTGTGTTCATCAT	168
			GCACTTCTTGACGATGTTCTTGC	
3	*KEAP-1*	NM_016679	TGCCCCTGTGGTCAAAGT	104
			GGTTCGGTTACCGTCCTGC	
4	*NFkb*	NM_008689	CCACGCTCAGCTTGTGAGGGAT	106
			GGCCAAGTGCAGAGGTGTCTGAT	
5	*NRF2*	NM_010902	CTCGCTGGAAAAAGAAGTG	240
			CCGTCCAGGAGTTCAGAGG	
6	*Catalase*	NM_009804	AGCGACCAGATGAAGCAGTG	181
			TCCGCTCTCTGTCAAAGTGTG	
7	*SOD2*	NM_013671	GCGGTCGTGTAAACCTCAT	240
			CCAGAGCCTCGTGGTACTTC	
8	*Prx6*	NM_007453	TAAGGACAGGGACATTTCCATCC	145
			CCGTGGAGTTAGGGTAGAGGA	
9	*Xrcc4*	NM_028012	GAGACACCGAATGCAGAAGA	121
			GGTGCTCTCCTCTTTCAAGG	
10	*Xrcc5*	NM_009533	GAAGAACAGCGCTTCAACAG	92
			TCCTGAACAACAATTTCCCA	
11	*LigIV*	NM_176953	ATGGCTTCCTCACAAACTTCAC	103
			TTTCTGCACGGTCTTTACCTTT	
12	*TNFa*	NM_013693	ATGAGAAGTTCCCAAATGGC	125
			CTCCACTTGGTGGTTTGCTA	
13	*AP-1*	NM_010591	CACGGAGAAGAAGCTCACAA	126
			ACTTGTTACCGGTCCTCTGG	
14	*Ki67*	NM_001081117	ATCATTGACCGCTCCTTTAGGT	104
			GCTCGCCTTGATGGTTCCT	
15	*IL6*	NM_031168	TAGTCCTTCCTACCCCAATTTCC	76
			TTGGTCCTTAGCCACTCCTTC	

sia) supplemented by 10% (primary cell cultures and L-929 line) or 20% (HL-60 line) embryonic bovine serum (Gibco, USA), 2 mM L-glutamine, 100 U/ml penicillin, and 100 μg/ml streptomycin (PanEco, Russia), at 37 °C and 5% carbon dioxide atmosphere in a CO_2 incubator (Binder, Germany). Initially cells 3×10^4 cells/dish in 3 ml were placed in Petri dishes Ø 35 mm. 10^{10}/ml Se NP, 0.5 mg/ml IgG or a combination thereof were added in appropriate samples. The cells were cultured for 3 days. After incubation cells were rinsed 3 times by BPS and stained with fluorescent dyes 2 micrograms/ml Hoechst 33342 (Sigma, USA) and 2 micrograms/ml propidium iodide (Sigma, USA) to determine the number of living and dead cells, respectively. Hoechst 33342 stains all cells (living and dead). Propidium iodide dye penetrates into living cells extremely slowly, so in a short incubation time (we used about 10 minutes) it stains only cells with a damaged plasma membrane. A plasma membrane with ruptures leading to dye penetration was one of the main criteria for cell death. Microscopic analysis of the samples was carried out using an imaging system based on Leica DMI6000 (Leica, Germany). ImageJ (HIN,

USA) was used to data analysis. Survival, cells area and area of the nucleus were calculated. At least 500 cells were analyzed on the surface of each sample for analysis.

Gene expression

Real-time RT PCR was applied to analyze gene expression in surviving murine granulocytes cultures. Total RNA from cells was extracted using ExtractRNA reagent. The quality of RNA was assessed by electrophoresis in 2% agarose gel in TAE buffer in the presence of ethidium bromide (1 μg/ml). RNA concentration was measured on NanoDrop 1200c spectrophotometer (Metler Nolledo, USA). To avoid possible contamination with genomic DNA, the isolated RNA was treated with RQ1 DNAse. For reverse transcription (RT) 2 μg of total RNA was used with MMLV RT kit. The obtained cDNA was subsequently used in PCR with gene-specific primers (Table 1) synthesized by "Evrogen" (Russia). Real-time PCR was run in thermocycler QuantStudio 5 (Thermo Fisher Scientific, USA) using qPCRmix-HS kit, which contains fluorescent intercalating dye SYBR Green II. Results were calculated according to a standard method. All details have been previously described (Sharapov *et al.*, 2020).

Assay of IgG solutions optical properties

Absorption spectra were measured on a Cintra 4040 (GBC Cintra 4040, Australia) in quartz cuvettes with an optical path length of 10 mm at room temperature (~22 °C). The BSA concentration was 0.5 g/L. The absorption spectra were measured with at least 6 samples for each group.

Hydrodynamic particle diameters was evaluated by dynamic light scattering (DLS) with Zetasizer ULTRA Red Label (Malvern Panalytical Ltd., Malvern, UK). A 1 ml solution of IgG with a concentration of 5 mg/ml was measured in a plastic cuvette at 25 °C. Five independent experiments were carried out for the control and samples with different Se NPs concentration. The intensity distributions of the hydrodynamic diameters were calculated using the ZS Xplorer program and algoritm (Penkov, 2020).

Fluorescence of samples in water was studied on a Jasco FP-8300 spectrometer (JASCO Applied Sciences, Canada). Measurements of a 2 ml solution of IgG with a protein concentration of 5 mg/ml were carried out in quartz cuvettes with an optical path length of 10 mm at room temperature (~25 °C). Each sample was measured in triplicate. The intensity maxima change by several percents (Sarimov *et al.*, 2021b).

Refractive index measurements were carried out on a Multiwavelengths Refracto-meter: Abbemat MW (Anton Paar, Graz, Austria). The IgG solution (5 mg/ml, 1 ml) was added into the cell of the device and measurements were made at a wavelength of 435.8, 589.3 and 632.8 nm at a temperature of 25 °C (Nagaev *et al.*, 2022).

Statistics

Statistical processing was performed with Sigma Plot and MS Office Excel software. All data were presented as mean ± standard error. At least 3 independent experiments were carried out for each study conditions. The statistical significance of differences between the samples was assessed using the Mann-Whitney test or signed rank test (Z-statistic).

Results

Se NPs were obtained by laser ablation with further laser ablation fragments to obtain the narrowest possible size distribution. During laser fragmentation of nanoparticles, the characteristic processes occurring in the experimental cell were controlled by recording acoustic oscillations and the nature of plasma formation (Fig. 1). It is shown that the dependence of amplitude of acoustic oscillations on Se NPs concentration can be approximated by two linear functions in the presented coordinates (Fig. 1a). The first is in the concentration range from 5×10^6 to 10^8 NPs ml, the second is in the concentration range from 10^8 to 10^{10} NPs/ml. The interpolation accuracy will be quite high due to the small measurement variability. The optical changes in the experimental cuvette during laser fragmentation can be described by one linear function in the presented coordinates (Fig. 2b), but not by two functions. This phenomenon

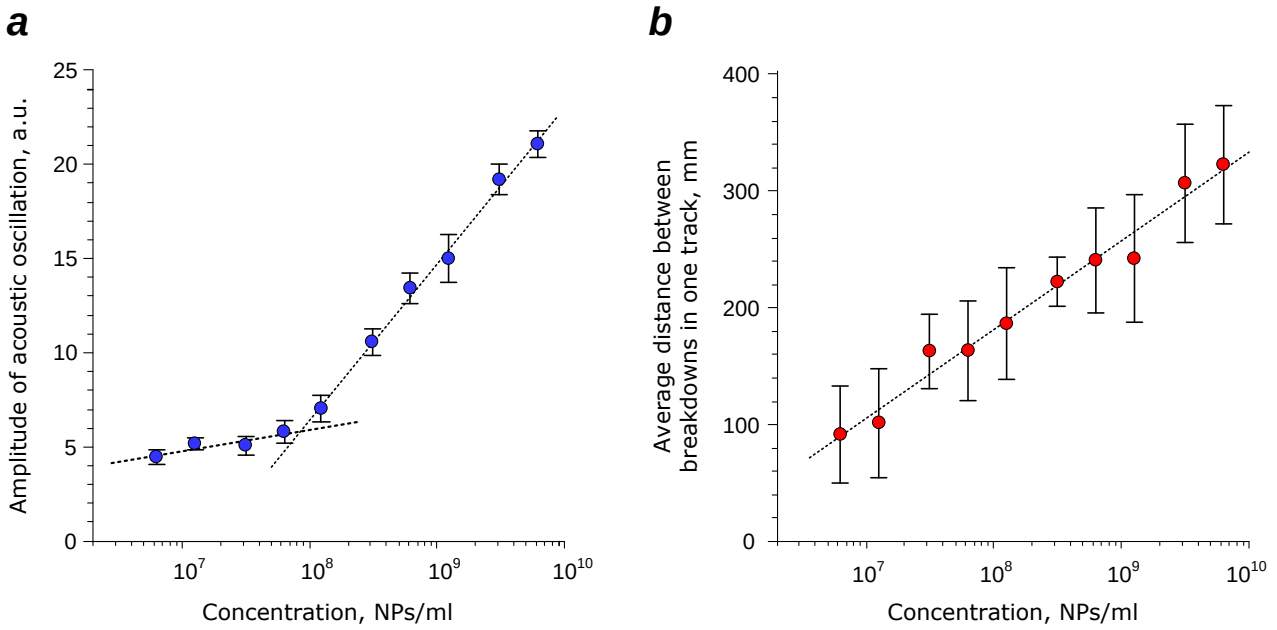

Fig. 1. Dependence of acoustic oscillations amplitude (a) and average distance between optical breakdowns at laser fragmentation (b) on Se NPs concentration. Data are presented as means ± SE (n = 3). The dotted lines show the linear approximation

is unusual to NPs colloids. The interpolation accuracy will be somewhat lower.

We achieved rather narrow size evolution of Se NPs via controlling the physicochemical processes in the experimental cell (Fig. 2a). The obtained Se NPs were studied using the dynamic light scattering method. Average hydrodynamic diameter of Se NPs is about 100 nm. The half-width of size distribution is about 35 nm (70-105). TEM-assisted data support these results (Fig. 2b).

Cytotoxicity of Se NPs was studied (Fig. 3). Se NPs in concentrations 10^7-10^{11} did not change number of non-viable cell in case of primary cultures fibroblasts (Fig. 3a), hepatocytes (Fig. 3b) and epithelial-like L-929 cells (Fig. 3c).

Se NPs had weak cytotoxic effect against granulocyte-like cells LH-60 (Fig. 4d). Se NPs dose-dependent increase amount of non-viable cells from 5% (control) to 9 and 15% at Se NPs 10^{10}/ml and 10^{11}/ml respectively

It has been established that after addition of Se NPs decrease area of nucleus in L-929 and HL60 cells (Fig. 4). In L-929 cell culture reduction (about 15% compare with control) of nucleus area began from concentration 10^{10} NPs/ml. The HL60 cells were more sensitive to Se NPs. Addition of 10^8 NPs/ml reduced nucleus area on 25–30% compare with control (Fig. 4b). At concentrations 10^{10} and 10^{11} NPs/ml similar effect was observed.

As shown earlier Se NPs had more pronounced effect against granulocyte-like HL-60 cell line. Tendency to a decrease in viability was observed at 10^8 NPs/ml. Separately, experiments were carried out on a surviving culture of murine granulocytes. It was shown that no loss of viability was observed even at a concentration of 10^{11} NPs/ml. We proposed that mature granulocytes are more resistant to environmental changes than progenitor cells. The question arises whether nanoparticles can affect progenitor cells *in vivo* (red bone marrow cells).

Micronuclear test was carried out to evaluate Se NPs influence on progenitor blood cells (Fig. 5).

We observed that Se NPs up to 10^{10}/ml did not affect the formation of micronuclei, although there is a tendency to increase the num-

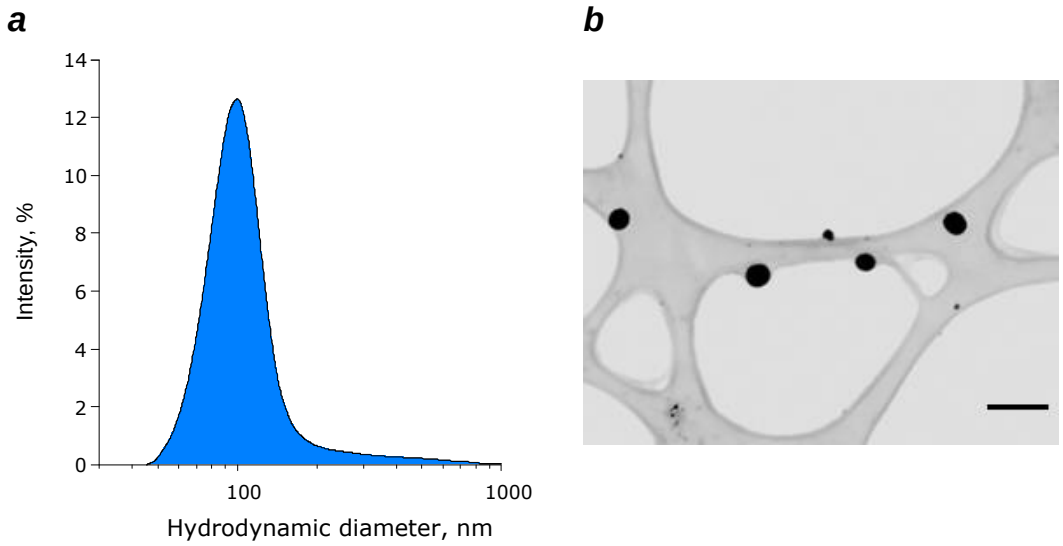

Fig. 2. Distribution of Se NPs by size obtained by DLS (a). TEM-image of individual Se NPs (b). Scale bar is 200 nm

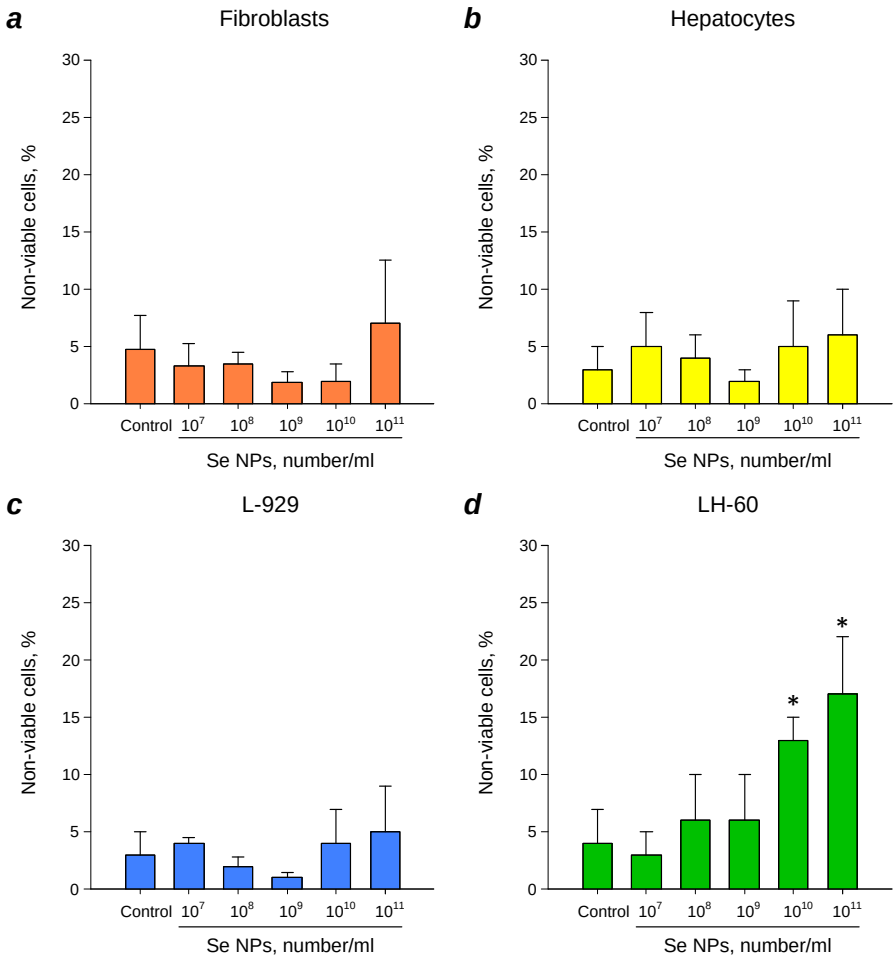

Fig. 3. Influence of Se NPs in different concentrations on number of non-viable cells in primary cultures of fibroblasts (a) and hepatocytes (b), cell lines lines L-929 (c) and LH-60 (d). Results are presented as means ± standard errors (n = 5). * – $p < 0.05$, compared with control, Mann-Whitney test

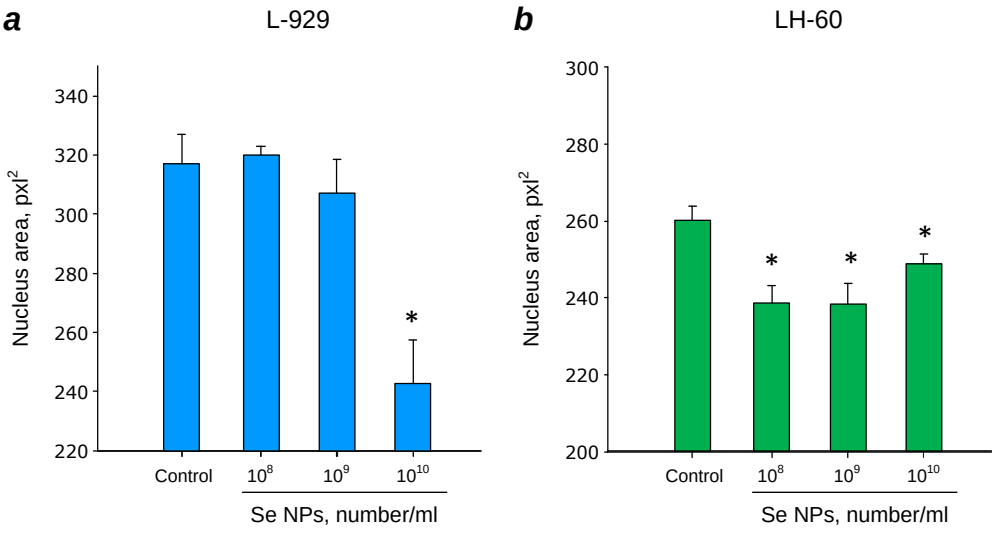

Fig. 4. Influence of Se NPs in different concentrations on nucleus area in L-929 (a) and LH-60 (b) cell lines. Results are presented as means ± standard errors (n = 5). * – $p < 0.05$, compared with control, Mann-Whitney test

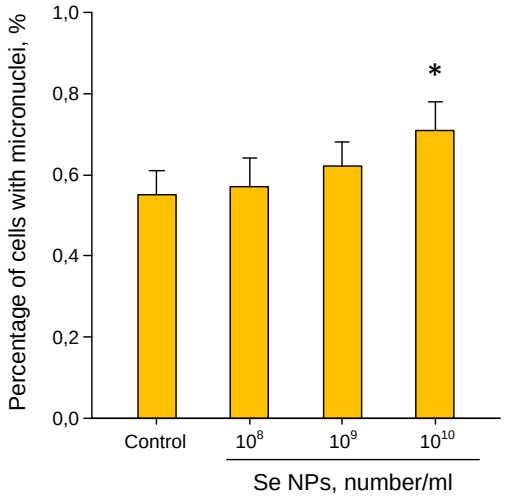

Fig. 5. The effect of Se NPs injected intravenously on the formation of polychromatophilic red cells with micronuclei in the red bone marrow of mice. The data are presented as average values ± standard error (n = 5). * – $p < 0.05$, compared with control, Mann-Whitney test

ber of cells containing micronuclei. The percentage of cells with micronuclei increased by 12% relative to the control at a concentration of 10^{10} NPs/ml. At the concentration of 10^{11} NPs/ml, the number of cells with micronuclei increased by almost 20% ($p < 0.05$). Thus, Se NPs cannot affect normal granulocytes, while had moderate cytotoxic activity against myeloid granulocyte progenitor cells and granulocyte-like cell line.

Granulocytes as other innate immune cell play a role of "first line of defense" of the host. The main functions of granulocytes are the elimination of bacteria or other pathogen by generating ROS in the site of infection. Therefore, the effect of Se NPs on the rate of ROS generation by murine bone marrow granulocytes was researched. Recently, a lot of information has appeared in the literature about the interaction of granulocytes with antibodies, therefore, we studied effects of Se NPs and their combination with IgG immunoglobulin. The addition of Se NPs did not change base production of ROS by granulocytes (Table 2). Addi-

Table 2

Quantitative characteristics of the «respiratory burst» of murine bone marrow granulocytes caused by 1 μm Wp or 1 μm PMA

Parameter	PBS	Se NP 10^{10}/ml	Se NP 10^{10}/ml + + 0.5 mg/ml IgG	0.5 mg/ml IgG
Base level, a.u. (before stimulus)	1.7 ± 0.3	1.8 ± 0.3	4.1 ± 0.9 *§	3.9 ± 0.8 *§
Wp 1 μM				
Maximum amplitude, %	100	97 ± 4	118 ± 6 *§	119 ± 2 *§
ROS production (Integral Wp 100s/Integral base 100s)	5.7 ± 0.4	5.9 ± 0.3	5.2 ± 0.1	6.4 ± 0.2
PMA 1 μM				
Maximum amplitude, %	100	121 ± 18	55 ± 19 *§	66 ± 18 *§
ROS production (Integral PMA 100s/Integral base 100s)	21.9 ± 4.5	23.4 ± 5.6	2.8 ± 0.9 *§	3.7 ± 1.3 *§

Note: * – $p < 0.05$, compared with stimulus on the background of PBS, one-sample signed rank test Z-statistical ($n = 4$). § – $p < 0.05$, compared with stimulus on the background of Se NP 10^{10}/ml, Mann-Whitney test ($n = 4$).

tion IgG or combination of IgG with Se NPs increased base level of ROS generation (Table 2). Se NPs did not significantly modify the Wp- or PMA-induced respiratory burst of granulocytes (Fig. 6, Table 2). The addition of IgG did not change the total production of ROS (Fig. 6b), but increased the maximum amplitude of the response (Fig. 6a, Table 2).

The combination of IgG with Se NPs also enhanced the maximum amplitude of Wp-induced ROS generation (Fig. 6a, Table 2), but did not change the total ROS generation in 250 seconds (Table 2). The effect of combination of Se NPs + IgG on Wp-induced ROS generation was equal to influence of IgG added alone (Fig. 6a, Table 2). Se NPs did not change of maximum amplitude and total PMA-induced ROS generation by granulocytes (Fig. 6b, Table 2). The addition of combination Se NPs+IgG or IgG desreasesd total PMA-induced ROS production and maximum ROS generation (Fig. 6b, Table 2). The presence of Se NPs did not modify the PMA-induced ROS generation in the presence of IgG. The addition of IgG or Se NPs+IgG independently increased the basic production of ROS (Table 2). However, as in the case of a response to PMA, there were no synergistic effects between Se NPs and IgG, therefore, in both cases the effect is due to IgG.

Intracellular calcium plays an important role in regulating the functioning of granulocytes, therefore, at the next stage of the study, we evaluated the effects of IgG and Se NPs on the calcium activity of granulocytes at rest and in response to a pro-inflammatory stimulus, the W-peptide (Wp).

In base state after PBS application ~10% of granulocytes generated calcium spikes (Fig. 7a), other 90% cell stay “silent”. The addition of Se NPs addition, both with and without the addition of IgG, did not change the number of cells with calcium spikes in base conditions (Fig. 7b). IgG supplementation reduced the number of cells with calcium spikes in base conditions compared to controls. The addition of the «respiratory burst» inducer Wp increased the number of cells with calcium spikes in tree times compared to the control. The addition of Se NPs reduced the number of cells responding to Wp by up to ~10%. IgG did not affect the

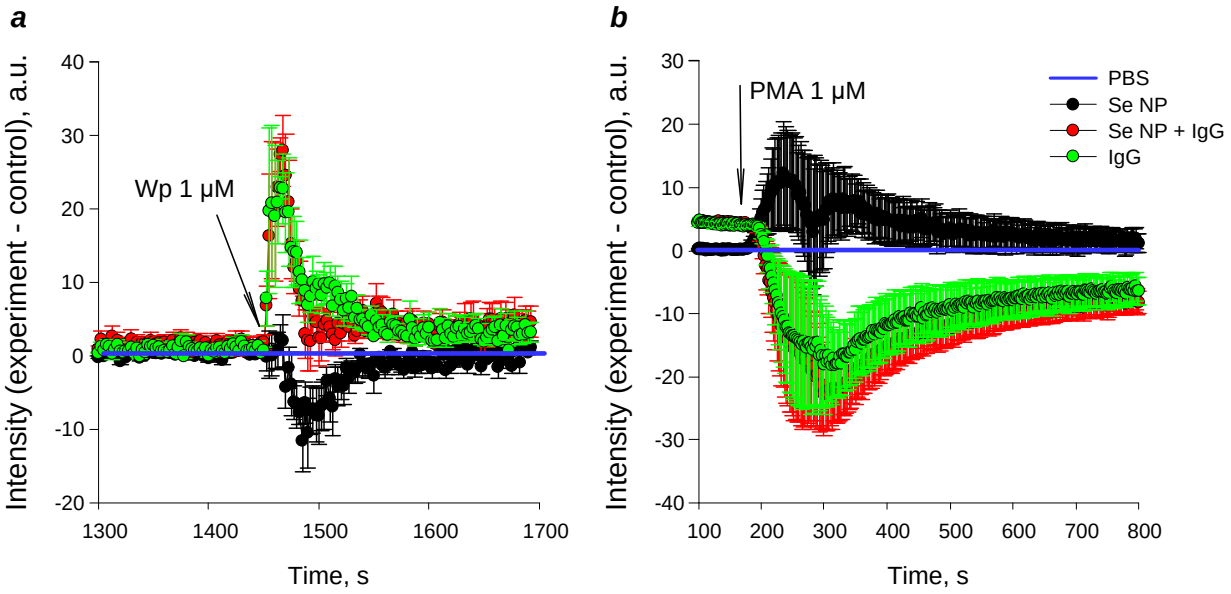

Fig. 6. The effect of Se NPs (10^{10}/ml) and/or IgG (0.5 mg/ml) on ROS production by murine bone marrow granulocytes in response to 1 μm Wp (a) or 1 μm PMA (b). The data are presented as a difference in chemiluminescence intensity in different experimental variants (Se NP 10^{10} NPs/ml, IgG 0.5 mg/ml or their combination) and intensity values obtained in control (PBS, blue line). The addition times of the corresponding substances are shown by arrows. All data is presented as Mean ± SE (n = 4)

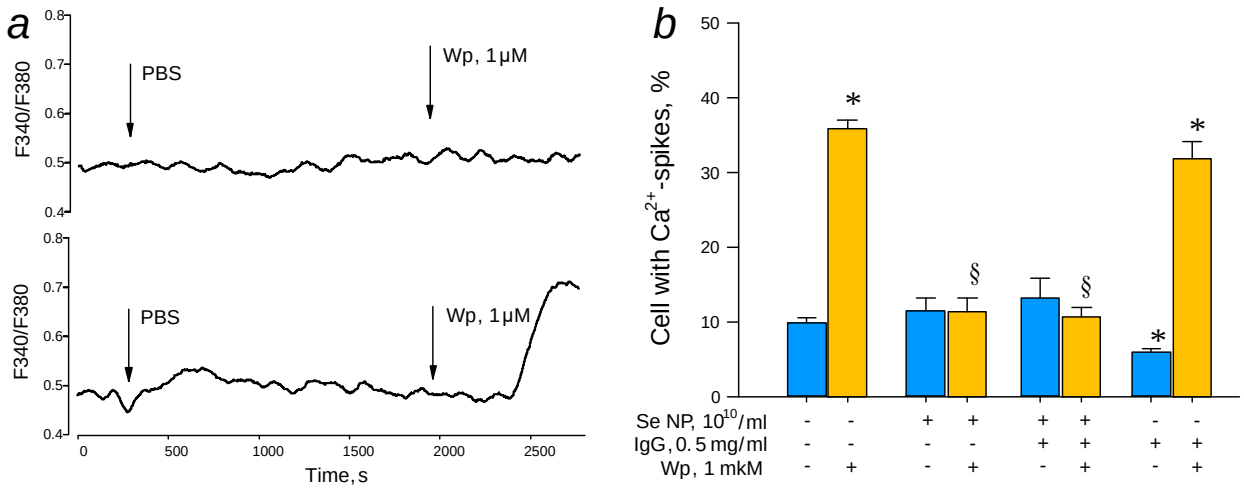

Fig. 7. Evaluation of calcium activity of murine bone marrow granulocytes. (a) Examples of typical individual records: cell without calcium response to stimulus Wp 1 μM (top) and cell response to Wp 1 μM (bottom). The amount of cytoplasmic calcium is proportional to the F340/F380 ratio. (b) proportions of cells with calcium responses in different variants of the experiment. Blue bar correspond to the proportions of cells with calcium activity in response to PBS, Se NP, IgG or their combination before addition of Wp. Orange bar correspond to proportions of cells with calcium activity after addition of Wp. Data are presented as Mean ± SE (n = 4). * – $p < 0.05$, compared with PBS without, Mann-Whitney test (n = 6). § – $p < 0.05$, compared with Wp 1 μM against the background of PBS, Mann-Whitney test (n = 6).

calcium activity of granulocytes to Wp. The effects of Se NPs with IgG combination and Se NPs on calcium activity of murine granulocytes were same.

Our results indicate that Se NPs are able to modulate the functional response of granulocytes against the background of IgG. Commonly, such effects are associated with the ef-

fects on the intracellular signaling mechanisms. We study cell expression profile of granulocytes in presence of IgG, Se NPs or their combination. The main results are presented in Fig. 8.

Incubation of granulocytes with Se NP at a concentration of 10^{10}/ml during 24 hours changed expression level of most studied genes weakly (between 25 and 50%) (Fig. 8). However, expression of some genes changed more noticeably. Expression of genes *HSP90*, *SOD2* and *NRF2* genes increased by 3, 4 and 7 times respectively. We proposed that the introduction of Se NPs leads to an increase in intracellular redox homeostasis, which is associated with an increase in the level of *NRF2*, which play important role in regulation of cell antioxidant response. In addition, *NRF2* levels can be increased by elevation of *NF-κB* levels. Expression of *NF-κB* significantly elevated 24 hours after Se NP administration. Increasing of expression level of *NF-κB* can also lead to increase of the expression level of *IL-6*. Changes in levels were much less pronounced and often did not differ from control values. Noticeable changes of expression of all studied genes were observed at Se NPs concentrations of 10^{10}/ml. Administration of Se NPs at concentrations of 10^{9}/ml did not change gene expression level (data not shown).

Incubation of granulocytes with Se NPs at a concentration of 10^{10}/ml during 24 hours changed expression level of most studied genes weakly (between 25 and 50%) (Fig. 8). However, expression of some genes changed more noticeably. Expression of genes *HSP90*, *HO-1* and *Catalase* genes increased by 2.5, 7 and 6 times respectively.

Administration of combination of Se NPs with IgG during 24 hours changed the expression level of most granulocyte genes. The expression level of the *SOD2* and *HSP90* genes increases 6 and 4 times respectively. The expression levels of *NFkb*, *IL6*, *Xrcc4* and *Xrcc5* increased by >2 times. Expression of the *HO-1* was decreased in ~2 times. Interestingly, direction of effects of combination Se NPs and IgG usually coincides with effect of Se NPs, but is numerically significantly different from the effect Se NPs without IgG. For example, the effect of the combination Se NPs with IgG is greater than the addition of Se NPs alone for *SOD2* by 50%, for *NF-κB* by 45%, for *IL6* by 60%, for *Xrcc4* and *Xrcc5* by more than 50%. At the same time, when one IgG was added for these genes, a decrease in the level of expression was observed. Thus, IgG enhances the effect of Se NPs, while IgG itself leads to a decrease in the level of expression. Based on the data obtained, we assume that Se NPs and IgG can interact with each other.

To test the assumption about the interaction of IgG and Se NPs molecules, we performed a study using optical methods of analysis.

The influence of Se NPs at concentrations of 10^{9}-10^{11}/ml on the optical absorption of IgG in solution was investigated (Fig. 9a). Se NPs in concentration of 10^{9}-10^{10}/ml increased absorption at local maximum ~280 nm by about 5% compare with control. Se NPs in concentration of 10^{9}-10^{10}/ml did not change absorption of the IgG solution at wavelengths >300 nm. Se NPs in concentration of 10^{11}/ml increased absorption at a local maximum ~280 nm by more than 20% compare with control and increased absorption at wavelengths of more than >300 nm by 30–35%.

The effect of Se NPs (10^{9}-10^{11}/ml) on refractive index of IgG solution was researched (Fig. 9b). The refractive index was measured at three laser wavelengths of 435.8nm, 589.3nm and 632.9 nm. Addition of 10^{9}/ml Se NPs did not change of refractive index at all three wavelengths. The addition of 10^{10}/ml Se NPs reduced the refractive index by (6-8)×10^{-5} at all three wavelengths. The addition of 10^{11}/ml Se NPs decreased the refractive index by more than 10^{-3} at all three studied wavelengths.

Se NPs at a studied concentration did not significantly change the optical absorption and refractive index of IgG solutions. We study influence of Se NPs on the fluorescence of IgG molecules (Fig. 10a, b). We observed local maximum in fluorescence spectrum of solution of 0.5 mg/ml IgG at a wavelength close to 330 nm (327–329 nm) at excitation wavelength 280 nm (Fig 10a). The addition of Se NPs de creased in fluorescence intensity in region

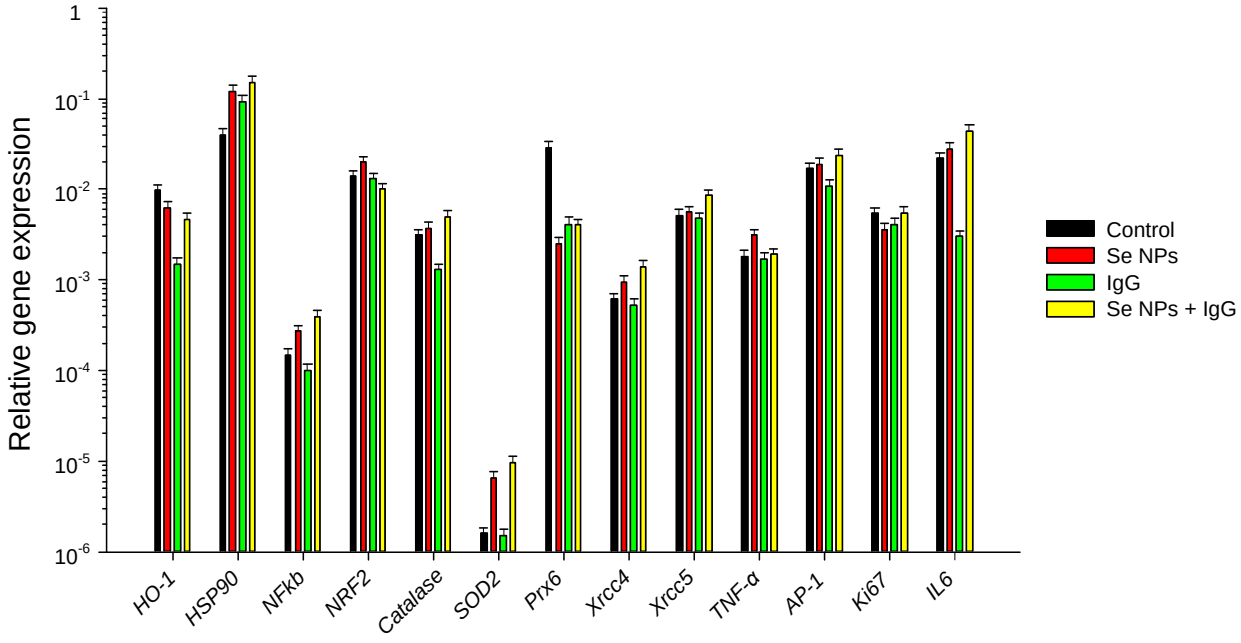

Fig. 8. Changes of the expression of stress-associated genes in granulocyte culture. The effect of the addition of Se NPs and/or IgG on the change in the amount of mRNA copies of corresponding genes after 24 hours. Changes in the number of mRNAs of the most variable genes ($P < 0.05$) relative to the expression level of the same genes in the control are presented. The average values are presented as mean ± SD (n = 5)

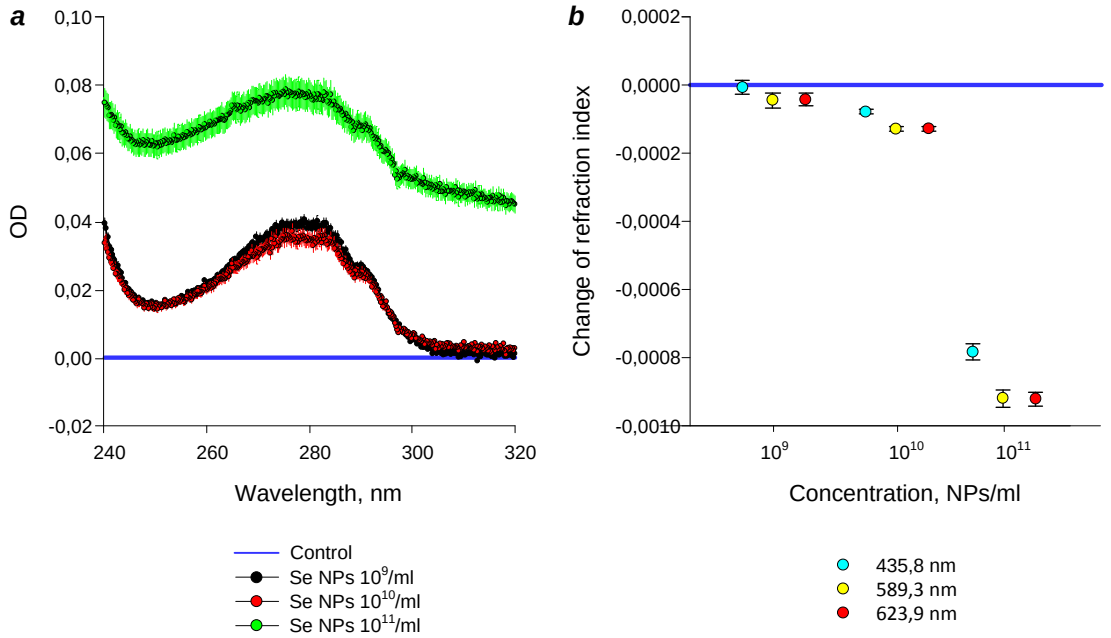

Fig. 9. The influence of Se NPs in different concentrations on the optical properties of IgG solution. (a). Optical absorption differences between IgG solutions with Se NPs 10^9-10^{10}/ml and IgG without Se NPs (contro, blue line). (b) Refractometry of IgG solutions containing and not containing Se NPs at wavelengths of 435.8 (cyan dots), 589.3 (yellow dots) and 632.9 (red dots) nm. All data is presented as Mean ± SE (n = 3)

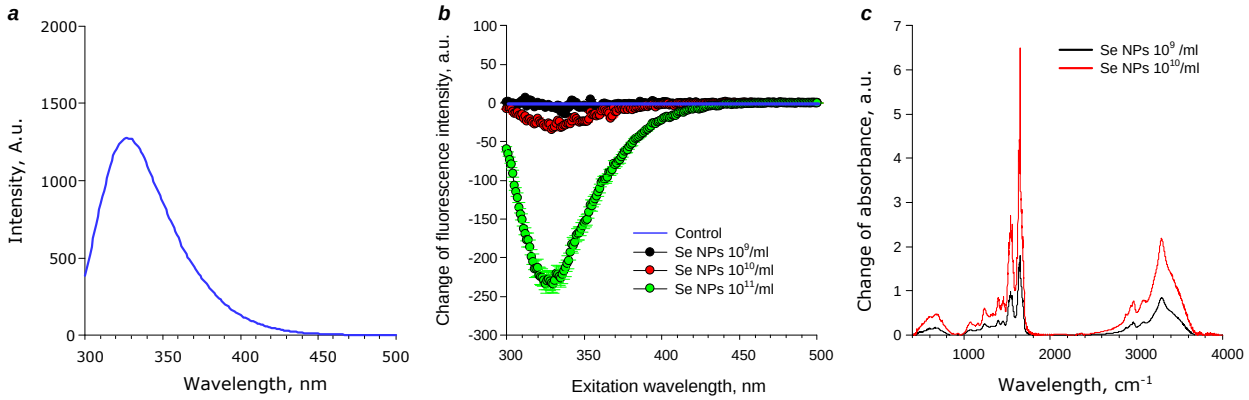

Fig. 10. The influence of Se NPs on fluorescence and the rotational–vibrational spectra of IgG. Fluorescence spectra of IgG in control (a). Differences between emission spectra of IgG solutions with Se NPs at concentrations 10^9-10^{11}/ml and control IgG solutions (without NPs, blue line) (b). All data is presented as Mean ± SE (n = 3). Influence of Se NPs at concentrations 10^9-10^{11}/ml on the rotational–vibrational spectra of aqueous IgG solutions. Data presented as differences between rotational–vibrational spectra of solutions IgG with Se NPs at concentrations 10^{10}-10^{11}/ml and rotational–vibrational spectra of control solution of IgG (without NPs)

Table 3

Size evolution of IgG in presence of Se NPs in different concentration or without NPs (control) obtained by DLS method

Peak	Hydrodynamic diameter, nm	Intensity, %
Control		
1	12.2	5.59 ± 0.46*
2	42.9	3.89 ± 0.73
Se NPs 10^{10}/ml		
1	13.1	2.97 ± 0.27
3	99.2	7.54 ± 2.12
Se NPs 10^{11}/ml		
1	106.4	16.07 ± 11.09
2	122.4	9.5 ± 8.4

Note: * – data is presented as Mean ± SE (n = 3).

310–330 nm in dose-dependent manner (Fig. 10b). Se NP 10^{10}/ml reduced fluorescence intensity decreased by >25 a.u. or ~2%. Se NP at concentration of 10^{11}/ml decreased fluorescence intensity by ~19%.

The effect of Se NPs on the change in the rotational–vibrational spectra of aqueous IgG solutions was studied (Fig. 10c). Se NPs significantly increases the IgG absorption in amide I (1650 cm-1) and amide II (1550 cm-1) bands. Administration of Se NP 10^{10}/ml lead to increasing of absorption intensity in amide I and amide II bands by ~4 and ~ 3 times respectively. Administration of Se NP 10^{11}/ml lead to increasing of absorption intensity in amide I and amide II bands by ~8 and ~ 2 times respectively (2 time more than 10^{10}/ml).

The influence of Se NPs on the size distribution of particles in IgG solutions was evaluated (Table 3). Two peaks ~12 nm and ~43 nm were detected in control IgG solution. First peak corresponds to individual molecules of IgG. Second peak corresponds to aggregates of IgG. New peak ~100 nm appeared after Se NPs administration. This peak corresponds to avarage size of Se NPs (Fig 2). Addition of 10^{10}/ml Se

NPs reduced amount of individual molecules IgG by ~40% and removed peak of IgG aggregates. In presence of 10^{11}/ml Se NPs peak of individual IgG was not found in a solution. Two-humped peak with maxima at ~110 and ~120 nm were found.

Discussion

In present work, Se NPs were synthesized by laser ablation with the subsequent by laser fragmentation. Two methods were used to control the fragmentation of Se NPs. The first method based on evaluation of acoustic oscillations amplitude (Fig. 1a). The second method based on determination of optical average distance between optical breakdowns (Fig. 1b). Using fragmentation control, we synthesized Se NPs with narrow range (~100 nm) of size distributions (Fig. 2).

Acute cytotoxicity of obtained Se NPs was tested (Fig. 3). Se NPs at concentration 10^7-10^{11} NPs/ml did not influence of cell viability in primary cultures of fibroblasts and hepatocytes, as well as to the epithelial-like cell line L-929 (Fig. 3a-c). Se NPs decreased cell viability in granulocyte-like culture HL-60 at concentrations 10^{10}-10^{11} NPs/ml (Fig. 2d). Obtained results indicate a difference of Se NPs cytotoxicity level between primary cultures and immortalized cell lines, as well as between two immortalized cell lines. Our results are consistent with literature data on the dependence of the toxicity of NPs of metals and metal oxides on cells line (Gudkov *et al.*, 2022a). In present day, way to increase toxicity of NPs of metals and their oxides against cancer cells and decrease toxicity of NPs against normal cells are searched (Gudkov *et al.*, 2022b). In this instance, the greater toxicity of Se NPs against the human leukemia cell line HL-60 compared to normal primary cultures of fibroblasts and hepatocytes makes Se NPs an interesting candidate for the role of a potencial anticancer agent. It is worth noting, that 10^{10}/ml is quite a high concentration. In this case, Se NPs take up ~10^{-5} part of all solution volume with calculated average distance of ~4.5 μm from each other. If a eukaryotic cell will have average dimensions 20×20×20 μm, ~100 nanoparticles with size 100 nm will contact with a it. It is believed that granulocyte progenitor cells are much more susceptible to the action of damaging factors (Lombaert *et al.*, 2006). The obtaining of micronuclei in cells after division is considered as a marker of DNA damage (Zaichkina *et al.*, 2004). The effect of Se NPs injected intravenously on the formation of polychromatophilic red cells with micronuclei in the red bone marrow of mice was studied (Fig. 5). Genotoxic effect of Se NPs was shown only at a concentration 10^{11}/ml. Thus, it has been shown that granulocyte-like cell culture, surviving granulocyte culture and myeloid granulocyte progenitor cells are quite resistant to the action of Se NPs, but interaction of Se NPs with cells is not excluded.

Granulocytes are a subpopulation of leucocytes. Granulocytes have large segmented nucleus and the presence of specific granules in the cytoplasm, the main functions of which are the generation of ROS «respiratory burst», phagocytosis of pathogens, regulation of adaptive immune response etc. (Cartwright *et al.*, 1964). It is obvious that before the loss of viability or damage to DNA occurs in granulocytes, a large number of signal-regulatory processes associated, including those with the generation of ROS (Bratton & Henson, 2011), must occur. Therefore we studied effect of Se NPs on ROS generation by bone marrow granulocytes. Different results were obtained on the effects of Se NP and IgG on the kinetics of ROS generation by murine granulocytes (Fig. 6, Table 2). The effect of combination of Se NP with IgG and individual IgG in the case of stimulation by Wp and PMA concurred. The effect of combination Se NP with IgG was more pronounced compared with individual IgG molecules. The influence of pure Se NP was opposite in sign. The administration of individual IgG increased the maximum amplitude Wp-induced ROS generation by murine granulocytes. This phenomenon may be explained by IgG-dependent cell priming (Khawaja *et al.*, 2019). The ability of antibodies to increase ROS production via FcγR receptors was described in the literature for human neutrophils and granulocytes from murine bone marrow (Fossati *et al.*, 2002;

Llewellyn *et al.*, 2014; Robinson *et al.*, 1992). In case PMA-induced "respiratory burst" we observed reduction of total ROs production in response to PMA after administration of IgG and IgG+Se NPs. Pure Se NPs did not significant change the total ROS production. The ability of antibodies to reduce «respiratory burst» is described to some rage of stimulus (include Wp) on the example of human fibroblasts (Napolitano *et al.*, 2018). The mechanism of this phenomenon stays unclear.

Considering the above, we proposed three possible explanation: 1). Se NPs do not interact with IgG. The functional activity of IgG does not change. In this case, the binding of Se NPs with IgG should completely neutralize the influence of Se NP; 2). IgG molecules completely «cover» the Se NPs. It must lead to elimination of Se NPs activity. This does not explain why the effect of combination of Se NP with IgG is greater than that of IgG; 3). IgG molecules interact with the Se NPs, «cover» they and change their properties and activities.

The effect of combination of Se NPs with IgG on the «respiratory burst» depended on the nature of stimulus. The maximum amplitude increased in the case of Wp. In the case of PMA, the total ROS production decreased. Wp is a specific ligand for high affinity receptors of formylated peptides (FPR2) (Christophe *et al.*, 2001; He & Ye, 2017). FPRs are metabotropic receptors associated with G-proteins (G protein-coupled receptor, GPCR), the activation of which leads to a variety of cell responses, including the assembly of active complex of NADH oxidase on the cell membrane, which is involved in synthesis of superoxide anion radical, which lead to generation of other ROS (Forsman *et al.*, 2011). PMA is a direct activator of protein kinase C (PKC). PKC is major intracellular signal molecule. Direct activation of PKC by PMA leads to functional responses of cells without participation of membrane GPCR receptors and cytoplasmic calcium (Belambri *et al.*, 2018). The results obtained suggest that Se NP + IgG or IgG modulate both the receptor-dependent «respiratory burst» stage and the its stage caused by PKC activation.

In the next stage of our work we evaluated the influence of Se NPs and/or IgG on calcium activity of granulocytes. In the control, about 10% of granulocytes generated calcium spikes (Fig. 7), which is consistent with the data of our previous studies and other authors (Jaconi *et al.*, 1988; Safronova *et al.*, 2021; Serov *et al.*, 2019). An increase in the concentration of cytoplasmic calcium in response to Wp is well described in the literature and is one of the mechanisms of its activity. Activation of FPRs in response to Wp leads to an increase in the level of cytoplasmic calcium through the GPCR-dependent activation of PLC-β, which leads to hydrolysis of PIP_2 to IP_3. IP_3 lead to opening of IP_3R calcium channels on the endoplasmic reticulum (Dahlgren *et al.*, 2020; Forsman & Dahlgren, 2010). We have found the ability of Se NPs to block Wp-induced calcium responses in mouse granulocytes. Se^{2+} cations are capable of block the IP_3-dependent release of Ca^{2+} from the cytoplasmic reticulum (Uğuz & Nazıroğlu, 2012; Zheng *et al.*, 2005).

Clearly, Se NPs can release Se^{2+} ions into the surrounding solution, but the concentrations of Se^{+} ions should be extremely low. At least, we did not register a decrease in the hydrodynamic radius of nanoparticles or their number with the measurement accuracy available to us during the entire period of work. Potentially, Se^{+} ions are able to inhibit calcium signaling of cells. Thus, selenium ions inhibit the calcium responses of mouse granulocytes to Wp, while not affecting Wp-induced ROS production. ROS production is regulated by Ca^{2+}-dependent and Ca^{2+}-independent pathways (Belambri *et al.*, 2018; Dahlgren *et al.*, 2020; Forsman & Dahlgren, 2010). Probably, Se NPs can be considered as a potential inhibitor of Ca^{2+}-dependent proinflammatory pathways, which allow maintaining the functional activity of immune cells during the treatment of pathological inflammatory processes. Thus, Se NPs are able to significantly modulate the immunogenic response of granulocytes against the background of IgG induction. It is usually assumed that such effects are associated with an influence on the signaling regulatory mechan-

isms of cells. For this, the cell expression profile was studied. The main results are presented in figure 8.

It is known from the literature that the levels of ROS generated by granulocytes affect the expression of genes associated with the development of inflammation. Main pathway, activation of nuclear transcription factor κB (NF-κB) (Hugejiletu *et al.*, 2013). This nuclear transcription factor is a pleiotropic regulator of a large number of genes associated with the development of immune and inflammatory responses (Li *et al.*, 2017). This is confirmed by changes in the expression level of genes involved in the regulation of inflammation, *TNF-α*, *IL6*, *NF-κB*. Probably, the increased level of NF-κB suppresses the expression of *NRF2*, as was shown earlier (Li *et al.*, 2008). This explains the decrease in the expression levels of genes responsible for the expression of antioxidant enzymes, except for *SOD2*. It is possible that a reduction in *SOD2* expression is associated with the level of *HSP90* expression, which, in turn, may also be associated with a change in *NF-κB* expression (Dabravolski *et al.*, 2022). It is known that an increasing of level of *TNF-α* expression occurs when exposed to Se NPS, and depends on the concentration of nanoparticles and exposure time (Liu *et al.*, 2017). It is believed, selenium decreases of expression levels of pro-inflammatory gene by inhibiting of MAP-kinase-depending signaling pathways (Javdani *et al.*, 2019). The addition of the IgG and combination of Se NPs with IgG to the cells also significantly affected the expression profile of many genes. Often, IgG enhances the effect of Se NPs, while IgG without Se NPs decreased the level of expression of some genes (Fig. 8). This fact can only be explained by the presence of interaction between Se NPs and proteins. Recall that the data on the respiratory burst could most simply explain the interaction of nanoparticles and protein molecules.

Using several optical methods, we examined the interaction of IgG molecules with Se NPs was analyzed. The increasing of optical density of IgG solutions is observed after Se NPs administration (Fig. 9a). On the one hand, an increase in optical density is observed in the absorption region of aromatic amino acid residues, mainly tryptophan, on the other hand, optical density increases in the long-wave region (after 310 nm) in case of concentration 10^{11} NPs/ml. This data indicate a change of protein structure (Sarimov *et al.*, 2021a) associated with partial denaturation, chemical modification, aggregation, and interaction with the nanoparticle (Biswas *et al.*, 2018). Partial denaturation leads to significant increase of the amount of water molecules in the hydration shell of the protein. In its turn, an increasing of amount of water molecules in the protein hydration shell changes the refractive index (Sarimov *et al.*, 2018). The refractive index was measured with high accuracy at three wavelengths (Fig. 9b). The decreasing of refractive index by (6-8) $\times$ $\times 10^{-5}$ was recorded in presence Se NPs 10^{11}/ml. The fluorescence of a solution containing IgG and Se NPs was evaluated (Fig. 10a, b). We observed a maximum fluorescence intensity at 276–279 nm which correspond to fluorescence maximum of aromatic amino acids (Teale & Weber, 1957). After Se NPs administration fluorescence intensity of IgG decreases, but fluorescence emission maximum does not change. This indicates that, in presence of Se NPs weak degradation of aromatic amino acid residues probably occurs. The FTIR data indicate (Fig. 10c) that the addition of Se NP leads to an increase in absorption in the amide I (1650 cm–1) and amide II (1550 cm–1) bands. This may indicate partial melting of the protein structure and its aggregation. The evolution of the sizes of light-scattering particles in an aqueous solution of Se NPs and IgG was studied by DLS method (Table 3). Administration of Se NPs nanoparticles at concentration of 10^{10}/ml reduced number of individual IgG molecules. Addition of Se NPs at concentration of 10^{11}/ml completely removed individual IgG molecules from the solution. After the addition of nanoparticles, shift of the peak of individual molecules to the region of smaller sizes did non observed. It indicates that, there is no damage to the polypeptide chain. The proportion of individual protein molecules after the addition of Se NPs is the light scattering intensity of individual protein molecules, but does not change po-

sition. No formation of aggregates not associated with nanoparticles is observed. In the case of adding nanoparticles at a concentration of 10^{11}/ml, the right shoulder with a size of about 150 nm appears in the size distribution. We proposed, it is a projection of a dimer of nanoparticles covered with antibodies ((110 nm + + 110 nm + 220 nm)/3 = 146 nm) (Bunkin *et al.*, 2016).

Thus, it can be argued that immunoglobulins interact with Se NPs. Antibodies bind to the surface of Se NPs and are present in solutions in such a bound form. At the same time, in a significant part of the antibodies, a partial change in the tertiary and secondary structure is observed. This behavior of antibodies and Se NPs makes it possible to explain the results obtained both at the level of granulocyte physiology and at the level of expression of genes.

Conclusion

In present work, we studied the cytotoxicity of Se NPs and their effect on gene expression and functional responses of granulocytes. Se NPs were obtained by laser ablation in water followed by fragmentation, had a narrow size distribution with an average size of 100 nm. The resulting nanoparticles do not show acute toxicity to primary cultures of fibroblasts and hepatocytes, as well as to the epithelial-like cell line L-929. Se NPs at concentrations of 10^{10} NPs/mL and more exhibited a weak cytotoxic effect on granulocyte-like HL-60 cultures. The genotoxic effect on myeloid progenitor cells was weak and manifested only at a concentration of 10^{10} NPs/ml. We found the ability of Se NPs to modulate ROS production and calcium activity of mouse granulocytes (expressed as the proportion of cells with calcium spikes upon Wp stimulation). At the same time, Se NPs can modulate the effect of IgG on the physiological responses of granulocytes. In the study of gene expression, similar patterns were found. Se NPs increased the expression of «stress associated» genes. Antibodies enhance the effect of Se NP, while IgG without the addition of nanoparticles leads to a decrease in the level of expression of the studied genes. This fact can be explained by the interaction between Se NPs and IgG. Using optical methods, we found that antibodies bind with Se NPs. Antibodies bind to the surface of Se NPs and are present in aqueous solutions in such bound form. At the same time, a partial change in the tertiary and secondary structure is observed in a significant part of IgG in solution.

Contribution: concept and research preparation – A.M.E. and S.D.A.; research planning – A.M.E. and R.V.E.; research conducting – S.D.A., T.I.V., K.V.V., B.S.V. and P.R.V.; writing and drafting of article – S.D.A., T.I.V., R.V.E. and K.V.V.; project administration – A.M.E. All authors have read and agreed with the published version of the manuscript.

Funding: this work was supported by a grant of the Ministry of Science and Higher Education of the Russian Federation (075-15-2022-315) for the organization and development of a Worldclass research center «Photonics».

References

BELAMBRI S.A., ROLAS L., RAAD H., HURTADO-NEDELEC M., DANG P.M.-C. & EL-BENNA J. (2018): NADPH oxidase activation in neutrophils: Role of the phosphorylation of its subunits. *European Journal of Clinical Investigation* **48**(S2), e12951. https://doi.org/10.1111/eci.12951.

BISWAS B., MUTTATHUKATTIL A.N., REDDY G. & SINGH P.C. (2018): Contrasting Effects of Guanidinium Chloride and Urea on the Activity and Unfolding of Lysozyme. *ACS Omega* **3**(10), 14119–14126. https://doi.org/10.1021/acsomega.8b01911.

BORA K.A., HASHMI S., ZULFIQAR F., ABIDEEN Z., ALI H., SIDDIQUI Z.S. & SIDDIQUE K.H.M. (2022): Recent progress in bio-mediated synthesis and applications of engineered nanomaterials for sustainable agriculture. *Frontiers in Plant Science* **13**. https://doi.org/10.3389/fpls.2022.999505.

BRATTON D.L. & HENSON P.M. (2011): Neutrophil clearance: when the party is over, clean-up begins. *Trends in Immunology* **32**(8), 350–357. https://doi.org/10.1016/j.it.2011.04.009.

BUNKIN N.F., SHKIRIN A.V., LYAKHOV G.A., KOBELEV A.V., PENKOV N.V., UGRAITSKAYA S.V. & JR. E.E.F. (2016): Droplet-like heterogeneity of aqueous tetrahydrofuran solutions at the submicrometer scale. *The Journal of Chemical Physics* **145**(18), 184501. https://doi.org/10.1063/1.4966187.

CARTWRIGHT G., ATHENS J. & WINTROBE M. (1964): Analytical review: The kinetics of granulopoiesis in normal man. *Blood* **24**(6), 780–803.

CHIU M.L., GOULET D.R., TEPLYAKOV A. & GILLILAND G.L. (2019): Antibody Structure and Function: The Basis for Engineering Therapeutics. *Antibodies* **8**(4), 55.

CHRISTOPHE T., KARLSSON A., DUGAVE C., RABIET M.J., BOULAY F. & DAHLGREN C. (2001): The synthetic peptide Trp-Lys-Tyr-Met-Val-Met-NH2 specifically activates neutrophils through FPRL1/lipoxin A4 receptors and is an agonist for the orphan monocyte-expressed chemoattractant receptor FPRL2. *J Biol Chem* **276**(24), 21585–21593. https://doi.org/10.1074/jbc.M007769200.

DABRAVOLSKI S.A., SUKHORUKOV V.N., KALMYKOV V.A., OREKHOV N.A., GRECHKO A.V. & OREKHOV A.N. (2022): Heat Shock Protein 90 as Therapeutic Target for CVDs and Heart Ageing. *International Journal of Molecular Sciences* **23**(2), 649.

DAHLGREN C., HOLDFELDT A., LIND S., MÅRTENSSON J., GABL M., BJÖRKMAN L., SUNDQVIST M. & FORSMAN H. (2020): Neutrophil Signaling That Challenges Dogmata of G Protein-Coupled Receptor Regulated Functions. *ACS Pharmacol Transl Sci* **3**(2), 203-220. https://doi.org/10.1021/acsptsci.0c00004.

DUNG N.T., TRONG T.D., VU N.T., BINH N.T., MINH T.T.L. & LUAN L.Q. (2021): Radiation Synthesis of Selenium Nanoparticles Capped with β-Glucan and Its Immunostimulant Activity in Cytoxan-Induced Immunosuppressed Mice. *Nanomaterials* **11**(9), 2439.

FERRO C., FLORINDO H.F. & SANTOS H.A. (2021): Selenium Nanoparticles for Biomedical Applications: From Development and Characterization to Therapeutics. *Advanced Healthcare Materials* **10**(16), 2100598. https://doi.org/https://doi.org/10.1002/adhm.202100598.

FILINA J.V., GABDOULKHAKOVA A.G. & SAFRONOVA V.G. (2014): RhoA/ROCK downregulates FPR2-mediated NADPH oxidase activation in mouse bone marrow granulocytes. *Cell Signal* **26**(10), 2138-2146. https://doi.org/10.1016/j.cellsig.2014.05.017.

FINGERHUT L., DOLZ G. & DE BUHR N. (2020): What Is the Evolutionary Fingerprint in Neutrophil Granulocytes? *International Journal of Molecular Sciences* **21**(12), 4523.

FORSMAN H. & DAHLGREN C. (2010): The FPR2-induced rise in cytosolic calcium in human neutrophils relies on an emptying of intracellular calcium stores and is inhibited by a gelsolin-derived PIP2-binding peptide. *BMC Cell Biol* **11**52. https://doi.org/10.1186/1471-2121-11-52.

FORSMAN H., KALDERÉN C., NORDIN A., NORDLING E., JENSEN A.J. & DAHLGREN C. (2011): Stable formyl peptide receptor agonists that activate the neutrophil NADPH-oxidase identified through screening of a compound library. *Biochem Pharmacol* **81**(3), 402–411. https://doi.org/10.1016/j.bcp.2010.11.005.

FOSSATI G., BUCKNALL R.C. & EDWARDS S.W. (2002): Insoluble and soluble immune complexes activate neutrophils by distinct activation mechanisms: changes in functional responses induced by priming with cytokines. *Ann Rheum Dis* **61**(1), 13-19. https://doi.org/10.1136/ard.61.1.13.

GÁL P., VARINSKÁ L., FÁBER L., NOVÁK Š., SZABO P., MITRENGOVÁ P., MIROSSAY A., MUČAJI P. & SMETANA K. (2017): How Signaling Molecules Regulate Tumor Microenvironment: Parallels to Wound Repair. *Molecules* **22**(11), 1818.

GALVÃO I., ATHAYDE R.M., PEREZ D.A., REIS A.C., REZENDE L., DE OLIVEIRA V.L.S., REZENDE B.M., GONÇALVES W.A., SOUSA L.P., TEIXEIRA M.M. & PINHO V. (2019): ROCK Inhibition Drives Resolution of Acute Inflammation by Enhancing Neutrophil Apoptosis. *Cells* **8**(9), 964.

GAO S., YANG X., XU J., QIU N. & ZHAI G. (2021): Nanotechnology for Boosting Cancer Immunotherapy and Remodeling Tumor Microenvironment: The Horizons in Cancer Treatment. *ACS Nano* **15**(8), 12567–12603. https://doi.org/10.1021/acsnano.1c02103.

GAUTAM P.K., KUMAR S., TOMAR M.S., SINGH R.K., ACHARYA A., KUMAR S. & RAM B. (2017): Selenium nanoparticles induce suppressed function of tumor associated macrophages and inhibit Dalton's lymphoma proliferation. *Biochemistry and Biophysics Reports* **12**172–184. https://doi.org/10.1016/j.bbrep.2017.09.005.

GUDKOV S.V., BURMISTROV D.E., SMIRNOVA V.V., SEMENOVA A.A. & LISITSYN A.B. (2022a): A Mini Review of Antibacterial Properties of Al_2O_3 Nanoparticles. *Nanomaterials (Basel)* **12**(15). https://doi.org/10.3390/nano12152635.

GUDKOV S.V., GUDKOVA O.Y., CHERNIKOV A.V. & BRUSKOV V.I. (2009): Protection of mice against X-ray injuries by the post-irradiation administration of guanosine and inosine. *International Journal of Radiation Biology* **85**(2), 116–125.

GUDKOV S.V., POPOVA N.R. & BRUSKOV V.I. (2015): Radioprotective substances: History, trends and prospects. *Biophysics* **60**(4), 659-667. https://doi.org/10.1134/S0006350915040120.

GUDKOV S.V., SEROV D.A., ASTASHEV M.E., SEMENOVA A.A. & LISITSYN A.B. (2022b): Ag_2O Nanoparticles as a Candidate for Antimicrobial Compounds of the New Generation. *Pharmaceuticals* **15**(8), 968.

GUILLIN O.M., VINDRY C., OHLMANN T. & CHAVATTE L. (2019): Selenium, Selenoproteins and Viral Infection. *Nutrients* **11**(9), 2101.

HAO L., MARSHALL A.J. & LIU L. (2020): Bam32/DAPP1-Dependent Neutrophil Reactive Oxygen Species in WKYMVm-Induced Microvascular Hyperpermeability. *Front Immunol* **11**1028. https://doi.org/10.3389/fimmu.2020.01028.

HE H.-Q. & YE R.D. (2017): The Formyl Peptide Receptors: Diversity of Ligands and Mechanism for Recognition. *Molecules* **22**(3), 455.

HOSNEDLOVA B., KEPINSKA M., SKALICKOVA S., FERNANDEZ C., RUTTKAY-NEDECKY B., PENG Q., BARON M., MELCOVA M., OPATRILOVA R. & ZIDKOVA J. (2018): Nano-selenium and its nanomedicine applications: a critical review. *International journal of nanomedicine* **13,** 2107.

HUGEJILETU H., BOBE G., VORACHEK W.R., GORMAN M.E., MOSHER W.D., PIRELLI G.J. & HALL J.A. (2013): Selenium Supplementation Alters Gene Expression Profiles Associated with Innate Immunity in Whole-Blood Neutrophils of Sheep. *Biological Trace Element Research* **154**(1), 28–44. https://doi.org/10.1007/s12011-013-9716-6.

JACONI M.E., RIVEST R.W., SCHLEGEL W., WOLLHEIM C.B., PITTET D. & LEW P.D. (1988): Spontaneous and chemoattractant-induced oscillations of cytosolic free calcium in single adherent human neutrophils. *Journal of Biological Chemistry* **263**(22), 10557–10560. https://doi.org/10.1016/S0021-9258(18)38006-2.

JANGHORBANI M., MARTIN R.F., KASPER L.J., SUN X.F. & YOUNG V.R. (1990): The selenite-exchangeable metabolic pool in humans: a new concept for the assessment of selenium status. *Am J Clin Nutr* **51**(4), 670-677. https://doi.org/10.1093/ajcn/51.4.670.

JAVDANI M., HABIBI A., SHIRIAN S., KOJOURI G.A. & HOSSEINI F. (2019): Effect of Selenium Nanoparticle Supplementation on Tissue Inflammation, Blood Cell Count, and IGF-1 Levels in Spinal Cord Injury-Induced Rats. *Biological Trace Element Research* **187**(1), 202–211. https://doi.org/10.1007/s12011-018-1371-5.

KANG H., SEO J., YANG E.-J. & CHOI I.-H. (2021): Silver Nanoparticles Induce Neutrophil Extracellular Traps Via Activation of PAD and Neutrophil Elastase. *Biomolecules* **11**(2), 317.

KHAWAJA A.A., PERICLEOUS C., RIPOLL V.M., PORTER J.C. & GILES I.P. (2019): Autoimmune rheumatic disease IgG has differential effects upon neutrophil integrin activation that is modulated by the endothelium. *Scientific Reports* **9**(1), 1283. https://doi.org/10.1038/s41598-018-37852-5.

KHURANA A., TEKULA S., SAIFI M.A., VENKATESH P. & GODUGU C. (2019): Therapeutic applications of selenium nanoparticles. *Biomedicine & Pharmacotherapy* **111**, 802–812. https://doi.org/10.1016/j.biopha.2018.12.146.

KUROPATKINA T., PAVLOVA O., GULYAEV M., PIROGOV Y., KHUTOROVA A., STVOLINSKY S., MEDVEDEVA N. & MEDVEDEV O. (2022): Sex-Dependent Protective Effect of Combined Application of Solubilized Ubiquinol and Selenium on Monocrotaline-Induced Pulmonary Hypertension in Wistar Rats. *Antioxidants* **11**(3), 549.

LEHMAN H.K. & SEGAL B.H. (2020): The role of neutrophils in host defense and disease. *Journal of Allergy and Clinical Immunology* **145**(6), 1535–1544.

LI W., KHOR T.O., XU C., SHEN G., JEONG W.-S., YU S. & KONG A.-N. (2008): Activation of Nrf2-antioxidant signaling attenuates NFκB-inflammatory response and elicits apoptosis. *Biochem Pharmacol* **76**(11), 1485-1489. https://doi.org/10.1016/j.bcp.2008.07.017.

LI X., XING M., CHEN M., ZHAO J., FAN R., ZHAO X., CAO C., YANG J., ZHANG Z. & XU S. (2017): Effects of selenium-lead interaction on the gene expression of inflammatory factors and selenoproteins in chicken neutrophils. *Ecotoxicology and Environmental Safety* **139**447-453. https://doi.org/10.1016/j.ecoenv.2017.02.017.

LIN A. & LORÉ K. (2017): Granulocytes: New Members of the Antigen-Presenting Cell Family. *Front Immunol* **8.** https://doi.org/10.3389/fimmu.2017.01781.

LIU J., YANG Y., ZENG X., BO L., JIANG S., DU X., XIE Y., JIANG R., ZHAO J. & SONG W. (2017): Investigation of selenium pretreatment in the attenuation of lung injury in rats induced by fine particulate matters. *Environmental Science and Pollution Research* **24**(4), 4008–4017. https://doi.org/10.1007/s11356-016-8173-0.

LLEWELLYN D., DE CASSAN S.C., WILLIAMS A.R., DOUGLAS A.D., FORBES E.K., ADAME-GALLEGOS J.R., SHI J., PLEASS R.J. & DRAPER S.J. (2014): Assessment of antibody-dependent respiratory burst activity from mouse neutrophils on Plasmodium yoelii malaria challenge outcome. *J Leukoc Biol* **95**(2), 369-382. https://doi.org/10.1189/jlb.0513274.

LOMBAERT I.M., WIERENGA P.K., KOK T., KAMPINGA H.H., DEHAAN G. & COPPES R.P. (2006): Mobilization of bone marrow stem cells by granulocyte colony-stimulating factor ameliorates radiation-induced damage to salivary glands. *Clinical Cancer Research* **12**(6), 1804–1812.

MAIYO F. & SINGH M. (2017): Selenium nanoparticles: Potential in cancer gene and drug delivery. *Nanomedicine* **12**(9), 1075–1089.

NAGAEV E.I., BAIMLER I.V., BARYSHEV A.S., ASTASHEV M.E. & GUDKOV S.V. (2022): Effect of Laser-Induced Optical Breakdown on the Structure of Bsa Molecules in Aqueous Solutions: An Optical Study. *Molecules* **27**(19), 6752.

NAPOLITANO F., ROSSI F.W., PESAPANE A., VARRICCHIO S., ILARDI G., MASCOLO M., STAIBANO S., LAVECCHIA A., RAGNO P., SELLERI C., MARONE G., MATUCCI-CERINIC M., DE PAULIS A. & MONTUORI N. (2018): N-Formyl Peptide Receptors Induce Radical Oxygen Production in Fibroblasts Derived From Systemic Sclerosis by Interacting With a Cleaved Form of Urokinase Receptor. *Front Immunol* **9**574. https://doi.org/10.3389/fimmu.2018.00574.

PEISELER M. & KUBES P. (2019): More friend than foe: the emerging role of neutrophils in tissue repair. *The Journal of clinical investigation* **129**(7), 2629–2639.

PENKOV N.V. (2020): Temporal Dynamics of the Scattering Properties of Deionized Water. *Physics of Wave Phenomena* **28**(2), 135–139. https://doi.org/10.3103/S1541308X20020132.

PHILLIPSON M. & KUBES P. (2011): The neutrophil in vascular inflammation. *Nature Medicine* **17**(11), 1381–1390. https://doi.org/10.1038/nm.2514.

PI J., SHEN L., YANG E., SHEN H., HUANG D., WANG R., HU C., JIN H., CAI H., CAI J., ZENG G. & CHEN Z.W. (2020): Macrophage-Targeted Isoniazid–Selenium Nanoparticles Promote Antimicrobial Immunity and Synergize Bactericidal Destruction of Tuberculosis Bacilli. *Angewandte Chemie International Edition* **59**(8), 3226–3234. https://doi.org/10.1002/anie.201912122.

PROSHIN A.N., ORLOVA M.A. & TROFIMOVA T.P. (2017): Biological activity of some sulfur- and selenium-containing spiro compounds. *Russian Chemical Bulletin* **66**(10), 1931–1933. https://doi.org/10.1007/s11172-017-1968-4.

ROBINSON J., WATSON F., BUCKNALL R. C. & EDWARDS S.W. (1992): Activation of neutrophil reactive-oxidant production by synovial fluid from patients with inflammatory joint disease. Soluble and insoluble immunoglobulin aggregates activate different pathways in primed and unprimed cells. *Biochem J* **286 (Pt 2)**(Pt 2), 345–351. https://doi.org/10.1042/bj2860345.

SAFRONOVA V.G., VULFIUS C.A., ASTASHEV M.E., TIKHONOVA I.V., SEROV D.A., JIROVA E.A., PERSHINA E.V., SENKO D.A., ZHMAK M.N. & KASHEVEROV I.E. (2021): α9α10 nicotinic acetylcholine receptors regulate murine bone marrow granulocyte functions. *Immunobiology* **226**(1), 152047.

SARIMOV R.M., BINHI V.N., MATVEEVA T.A., PENKOV N.V. & GUDKOV S.V. (2021a): Unfolding and Aggregation of Lysozyme under the Combined Action of Dithiothreitol and Guanidine Hydrochloride: Optical Studies. *International Journal of Molecular Sciences* **22**(5), 2710.

SARIMOV R.M., LEDNEV V.N., SIBIREV A.V. & GUDKOV S.V. (2021b): The Use of Fluorescence Spectra for the Detection of Scab and Rot in Fruit and Vegetable Crops. *Frontiers in Physics* **8**. https://doi.org/10.3389/fphy.2020.640887.

SARIMOV R.M., MATVEYEVA T.A. & BINHI V.N. (2018): Laser interferometry of the hydrolytic changes in protein solutions: the refractive index and hydration shells. *Journal of Biological Physics* **44**(3), 345–360. https://doi.org/10.1007/s10867-018-9494-7.

SEROV D., ASTASHEV M., TIKHONOVA I. & SAFRONOVA V. (2019): The Influence of Exogenous ATP on Functional Responses of Murine Bone Marrow Granulocytes. *BIOLOGICHESKIE MEMBRANY* **36**(6-7), 61–71.

SEROV D., TIKHONOVA I., SAFRONOVA V. & ASTASHEV M. (2021): Calcium activity in response to nAChR ligands in murine bone marrow granulocytes with different Gr-1 expression. *Cell Biology International* **45**(7), 1533–1545.

SHARAPOV M.G., NOVOSELOV V.I., FESENKO E.E., BRUSKOV V.I. & GUDKOV S.V. (2017): The role of peroxiredoxin 6 in neutralization of X-ray mediated oxidative stress: effects on gene expression, preservation of radiosensitive tissues and postradiation survival of animals. *Free Radical Research* **51**(2), 148–166. https://doi.org/10.1080/10715762.2017.1289377.

SHARAPOV M.G., NOVOSELOV V.I., SAMYGINA V.R., KONAREV P.V., MOLOCHKOV A.V., SEKIRIN A.B., BALKANOV A.S. & GUDKOV S.V. (2020): A chimeric recombinant protein with peroxidase and superoxide dismutase activities: Physico-chemical characterization and applicability to neutralize oxidative stress caused by ionizing radiation. *Biochemical Engineering Journal* **159**107603. https://doi.org/10.1016/j.bej.2020.107603.

SIDDIK M.A.B., VATSOS I.N., RAHMAN M.A. & PHAM H.D. (2022): Selenium-Enriched Spirulina (SeE-SP) Enhance Antioxidant Response, Immunity, and Disease Resistance in Juvenile Asian Seabass, Lates calcarifer. *Antioxidants* **11**(8), 1572.

SIMAKIN A.V., BAIMLER I.V., SMIRNOVA V.V., UVAROV O.V., KOZLOV V.A. & GUDKOV S.V. (2021): Evolution of the Size Distribution of Gold Nanoparticles under Laser Irradiation. *Physics of Wave Phenomena* **29**(2), 102–107. https://doi.org/10.3103/S1541308X21020126.

SOKOLOV A.V., KOSTEVICH V.A., VARFOLOMEEVA E.Y., GRIGORIEVA D.V., GORUDKO I.V., KOZLOV S.O., KUDRYAVTSEV I.V., MIKHALCHIK E.V., FILATOV M.V., CHERENKEVICH S.N., PANASENKO O.M., ARNHOLD J. & VASILYEV V.B. (2018): Capacity of ceruloplasmin to scavenge products of the respiratory burst of neutrophils is not altered by the products of reactions catalyzed by myeloperoxidase. *Biochem Cell Biol* **96**(4), 457–467. https://doi.org/10.1139/bcb-2017-0277.

STOIBER W., OBERMAYER A., STEINBACHER P. & KRAUTGARTNER W.-D. (2015): The Role of Reactive Oxygen Species (ROS) in the Formation of Extracellular Traps (ETs) in Humans. *Biomolecules* **5**(2), 702–723.

TEALE F.W.J. & WEBER G. (1957): Ultraviolet fluorescence of the aromatic amino acids. *Biochemical Journal* **65**(3), 476-482. https://doi.org/10.1042/bj0650476.

TUROVSKY E.A., TUROVSKAYA M.V., BEREZHNOV A.V., TOLMACHEVA A.V., KAIMACHNIKOV N.P., DOLGACHEVA L.P., ZINCHENKO V.P., MAEVSKII E.I. & DYNNIK V.V. (2012): Convergence of Ca2+ signaling pathways in adipocytes. The role of L-arginine and protein kinase G in generation of transient and periodic Ca2+ signals. *Biochemistry (Moscow) Supplement Series A: Membrane and Cell Biology* **6**(1), 35–44. https://doi.org/10.1134/S1990747811060158.

UĞUZ A.C. & NAZıROĞLU M. (2012): Effects of Selenium on Calcium Signaling and Apoptosis in Rat Dorsal Root Ganglion Neurons Induced by Oxidative Stress. *Neurochemical Research* **37**(8), 1631–1638. https://doi.org/10.1007/s11064-012-0758-5.

VARLAMOVA E.G., GOLTYAEV M.V., MAL'TSEVA V.N., TUROVSKY E.A., SARIMOV R.M., SIMAKIN A.V. & GUDKOV S.V. (2021a): Mechanisms of the Cytotoxic Effect of Selenium Nanoparticles in Different Human Cancer Cell Lines. *International Journal of Molecular Sciences* **22**(15), 7798.

VARLAMOVA E.G., TUROVSKY E.A., BABENKO V.A. & PLOTNIKOV E.Y. (2021b): The Mechanisms Underlying the Protective Action of Selenium Nanoparticles against Ischemia/Reoxygenation Are Mediated by the Activation of the Ca2+ Signaling System of Astrocytes and Reactive Astrogliosis. *International Journal of Molecular Sciences* **22**(23), 12825.

VARLAMOVA E.G., TUROVSKY E.A. & BLINOVA E.V. (2021c): Therapeutic Potential and Main Methods of Obtaining Selenium Nanoparticles. *International Journal of Molecular Sciences* **22**(19), 10808.

VEISA V., KALERE I., ZAKE T., STRELE I., MAKRECKA-KUKA M., UPMALE-ENGELA S., SKESTERS A., REZEBERGA D., LEJNIEKS A., PUDULE I., GRINBERGA D., VELIKA B., DAMBROVA M. & KONRADE I. (2021): Assessment of Iodine and Selenium Nutritional Status in Women of Reproductive Age in Latvia. *Medicina* **57**(11), 1211.

VINOLO M.A.R., RODRIGUES H.G., NACHBAR R.T. & CURI R. (2011): Regulation of Inflammation by Short Chain Fatty Acids. *Nutrients* **3**(10), 858-876.

XIA H., ZHANG L., DAI J., LIU X., ZHANG X., ZENG Z. & JIA Y. (2021): Effect of selenium and peroxynitrite on immune function of immature dendritic cells in humans. *Medical Science Monitor: International Medical Journal of Experimental and Clinical Research* **27**, e929004-929001.

ZAICHKINA S.I., ROZANOVA O.M., APTIKAEVA G.F., ACHMADIEVA A.C. & KLOKOV D.Y. (2004): Low Doses of Gamma-Radiation Induce Nonlinear Dose Responses in Mammalian and Plant Cells. *Nonlinearity in Biology, Toxicology, Medicine* **2**(3), 15401420490519861. https://doi.org/10.1080/15401420490519861.

ZENG Y., XIANG Y., SHENG R., TOMÁS H., RODRIGUES J., GU Z., ZHANG H., GONG Q. & LUO K. (2021): Polysaccharide-based nanomedicines for cancer immunotherapy: A review. *Bioactive Materials* **6**(10), 3358–3382. https://doi.org/10.1016/j.bioactmat.2021.03.008.

ZHANG L., XIA H., XIA K., LIU X., ZHANG X., DAI J., ZENG Z. & JIA Y. (2021): Selenium regulation of the immune function of dendritic cells in mice through the ERK, Akt and RhoA/ROCK pathways. *Biological Trace Element Research* **199**(9), 3360–3370.

ZHANG Y., JIN J., HUANG B., YING H., HE J. & JIANG L. (2022): Selenium Metabolism and Selenoproteins in Prokaryotes: A Bioinformatics Perspective. *Biomolecules* **12**(7), 917.

ZHENG Y., ZHONG L. & SHEN X. (2005): Effect of selenium-supplement on the calcium signaling in human endothelial cells. *J Cell Physiol* **205**(1), 97-106. https://doi.org/10.1002/jcp.20378.